§25. Optimum Material Design of Tungsten for Plasma Facing Component Using Numerical Simulation

Nogami, S. (Tohoku Univ.),
Tamura, H.

1. Introduction

The solution hardening strengthening and dispersion strengthening are effective to improve the mechanical properties of tungsten for plasma facing material. However, degradation of the thermal properties occurs due to these strengthening treatments. Therefore, the balancing between the improvement and degradation of these properties is essential for the optimum material design as the plasma facing material.

The numerical simulation of the plasma facing component considering the actual structure and loadings is considered to be one of the solutions for this issue. The objective of this study is the optimum material design of the tungsten and its alloys by those strengthening methods based on the numerical structural simulation of the plasma facing component by using the material database developed by Tohoku University.

2. Numerical simulation procedures

The finite element analysis of the ITER divertor was carried out using the mechanical and thermal properties experimental database of the pure tungsten (PW), potassium-doped tungsten (KW) and potassium -doped tungsten containing 3% rhenium (KW3R).

The solver for the finite element analysis was the ANSYS v.15.0. The bullet perfectly plastic behavior after the yield point was assumed for the tungsten body and the piping component fabricated by the CuCrZr and OFHC-Cu. The heat load up to 10~20 MW/m^2 for 10 s was inputted to the divertor top surface. The heat loading and cooling times were 10 s and 20 s, respectively. The temperature and pressure of the cooling water were 25^{o}C and 2 MPa, respectively[1)].

3. Results and discussion

Fig. 1 shows the stress in the Y-direction during and after heat loading of 20 MW/m^2 at selected points. Heat loading at 20 MW/m^2 induced high strain and stress at the top surface and near the W/OFHC-Cu interface of the pure W monoblock. After 20 MW/m^2 heat loading, residual tensile strain and stress were observed at the top surface because of plastic deformation by compressive strain during heat loading. Recrystallization occurred at the top surface region during 20 MW/m^2 heat loading, which was considered to aid in crack formation in this region. For 10 MW/m^2 heat loading, the strain and stress values during heat loading and the residual strain after heat loading were quite low compared to the 20 MW/m^2 heat loading case. Therefore, the probability of crack formation during 10 MW/m^2 heat loading was considered low. These results agreed well with the experimental results obtained by previous heat load experiments using small-scale mockups.

K-doped W and K-doped W-3%Re showed higher recrystallization resistances than pure W, although the lower thermal conductivity from the addition of 3% Re resulted in a higher surface temperature for this material during heat loading. The effect of K-bubble dispersion and 3% Re addition on thermal stress distribution during heat loading was not clearly observed. Because of the higher temperature at which recrystallization starts for K-doped W-3%Re and K-doped W, the probability of crack formation at the top surfaces of these materials might be lower compared to that in pure W.

In neutron irradiation conditions, K-doped W-3%Re is predicted to show better resistance to irradiation hardening than pure W and K-doped W. The results of this work suggested that the probability of crack formation after heat loading was higher than that during heat loading. Both recrystallization and irradiation embrittlement will be clearly observed at relatively low temperature regions, which might increase the probability of crack formation and propagation in the cooling phase during cyclic heat loading. Therefore, it is considered that the K-doped W-3%Re will show higher resistance to crack initiation and propagation by cyclic heat loading, because the resistances of the material to both recrystallization and irradiation embrittlement exceed those of pure W and K-doped W.

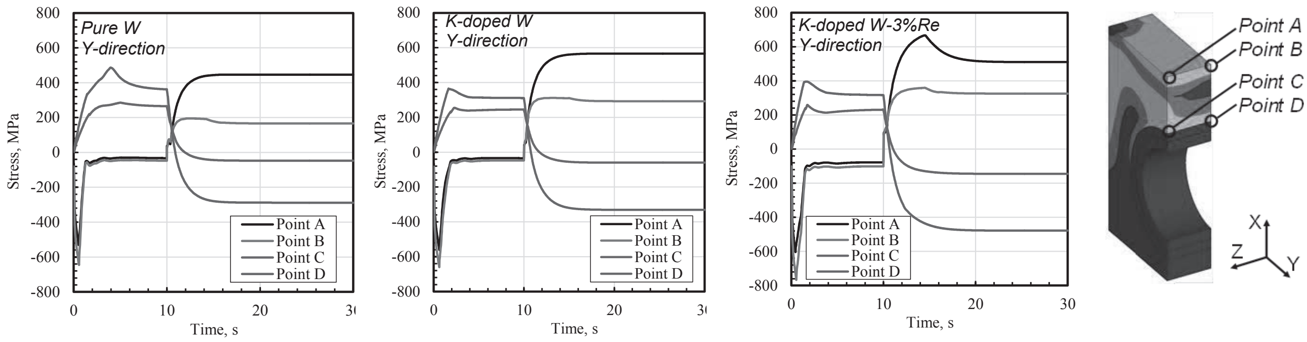

Fig. 1 Stress in the Y-direction during and after heat loading of 20 MW/m^2 at selected points.